Desalination and Water Treatment
www.deswater.com

doi: 10.5004/dwt.2018.22570

128 (2018) 20–26
October

Preparation and permeability of PVDF membranes functionalized with graphene oxide

Elwira Tomczak*, Martyna Blus

Faculty of Process and Environmental Engineering, Lodz University of Technology, Wolczanska 213/215, 90-924 Lodz, Poland, Tel. +48-42-6313708; email: elwira.tomczak@p.lodz.pl (E. Tomczak)

Received 8 March 2018; Accepted 8 May 2018

ABSTRACT

The study described in this paper aimed to develop a technology for producing polymeric membranes containing carbon nanostructures. The membranes were laboratory produced using commercial graphene oxide (GO) purchased from Sigma-Aldrich, USA. Polyvinylidene fluoride (PVDF) with and without (GO) ultrafiltration (UF) membranes was prepared via phase inversion process. The membrane support layer was made of polysulfone. The active layer containing GO was produced either by a spraying or by a mixing method. Several parameters, such as a thickness, the largest pore size, and tensile strength, were determined for the produced membranes. The addition of 0.002 wt% GO by mixing provided the hydrophilicity increase, which was expressed by the decrease of the contact angle of the membrane. A decrease in the mass transfer resistance of the PVDF/GO membrane with respect to the reference membrane (without GO) was observed. The tests related to water and bovine serum albumin (BSA) permeability were carried out with the Osmonics Koch laboratory UF device. The water volumetric flux (for ΔP = 0.6 MPa) through the membrane with GO disposed via spraying was lower (approaching J_v = 0.02 $m^3/(m^2\ h)$) than that of the membrane produced via mixing (approaching J_v = 0.12 $m^3/(m^2\ h)$). The former was almost the same as the one of the reference membrane. The retention coefficient for ΔP = 0.3–0.6 MPa and 1 g/dm^3 BSA solution was about 90%.

Keywords: Graphene oxide; Membrane composition; BSA; Ultrafiltration

1. Introduction

The first half of the 20th century is considered to be the beginning of the membrane manufacturing industry and J. Cadotte, the creator of composite membranes, main element of which has been a synthetic polymer. Nowadays, membrane manufacturing aims at creating layers as thin and selective as possible. Technologies employing "classic" polymeric membranes are already quite well mastered. The diversity of polymers possessing different properties has enabled the dynamic production of thin and selective membranes providing an efficient mass transfer. Membrane processes can be employed in many fields; however, the most important applications involve gas and liquid separations, such as water purification or concentration of dilute sewage in order to recover valuable substances. The former use seems necessary to ensure proper water resource management in the view of the global drinking water crisis [1,2]. The researches are also focused on the purification of water by removing heavy metal ions, hazardous dyes, pharmaceuticals and personal care compounds, and many others [3,4].

The membrane technology searches for materials allowing for ultrafast and efficient permeation. Researchers look not only for new polymers, but also mainly modify the existing materials through physical and even more often chemical processing.

In the last decade, a considerable attention has been paid to membranes functionalized with various nanoparticles [5–7] and carbon-derived nanomaterials, because of their availability, mechanical durability, and chemical resistance [8,9].

* Corresponding author.

Presented at the XII Scientific Conference "Membranes and Membrane Processes in Environmental Protection" – MEMPEP 2018 13–16 June 2018, Zakopane, Poland.

Carbon nanoparticles usually appear in the form of carbon nanotubes, graphene, and graphene oxide (GO) [10–12]. Initially, graphene has been the material of choice; however, manufacturing graphene has been so far very expensive. Hence, derivative materials, that is, carbon nanotubes and GO, are currently used [13,14]. The latter is much cheaper and easier to produce even with the support of a laboratory-scale technology, and most often via the Hummers' method [15]. Technical papers inform that polymeric membranes containing GO display hydrophilic properties, which result in increased water permeation and thereby more efficient separation of aqueous solutions [16–18]. These parameters are significantly influenced by the membrane production method [19–22]. Commercial membranes are usually made of several layers, including at least a support layer, a separation/skin layer, and a polymeric protective layer, but the addition of GO is the most important.

The review made by Hegab and Zou [23] provides not only a detailed update on the current GO-assisted desalination membranes, but also a discussion on how GO enhances the membrane efficiency. In addition, it presents the challenges facing GO-based membranes. According to the authors, modification of a membrane surface using GO can enhance several properties of membranes and it leads to the improvement of the antimicrobial effect, especially when GO on the membrane surface interacts directly with the bacterial cells. In addition, the GO membranes are more chlorine resistant, while maintaining the same reverse osmosis (RO) performance. The extra surface modification requires relatively small quantities of the nanomaterial (GO), which does not increase the environmental impact eventually caused by the production of GO. The authors discuss freestanding GO membranes, surface modification of the membranes using GO and GO-incorporated composite membranes. Additionally, they provide an overview regarding the recent researches on GO-based water desalination membranes including the membrane composition, fabrication methods, and membrane characteristics, for example, contact angle, flux, and contaminants rejection.

The structure and tunable physicochemical properties of GO offer an exciting opportunity to create a fundamentally new class of sieving membranes by stacking GO nanosheets. The nearly frictionless surface of GO facilitates the extremely fast flow of water molecules and strengthens the separation of aqueous solutions based on the molecular and the ionic sieving separation mechanisms [24].

Hosseini et al. [25] studied the performance of nanoporous GO while desalinating water with a RO membrane. The authors stated that the results concerning the hydrophilic functional groups on the surface of nanoporous membranes provided guidelines to design the next generation of nanomaterials for water desalination membranes. It was found that the water flux of nanoporous graphene oxide (NPGO) membranes was 2–5 orders of magnitude greater than that of other existing RO membranes. For all types of pores in NPGO membranes (pore radius between 2.9 and 4.5 Å) the salt rejection was greater than 89% and water flux was about 77% in comparison with the graphene membrane.

It is important to choose a suitable membrane-forming polymer. Wang et al. [26] used freestanding cellulose triacetate/GO (F-CTA/GO) membranes in a forward osmosis process. These membranes were fabricated using phase inversion. The authors achieved a significant ~68% increase in water flux (up to 18.43 L/m^2). The presence of 0.6 wt% GO provided an excellent mechanical stability of the freestanding membranes. The tensile strength and Young's modulus of the F-CTA/GO membrane increased to 42.8 MPa and 1.18 GPa, respectively, which corresponded to a ~84% and ~136% increase.

Tan et al. [27] examined the adsorptive properties of GO membranes. The adsorptive properties of Cu^{2+}, Cd^{2+}, and Ni^{2+} present on the GO membrane were systematically investigated using single, binary, and ternary solutions in batch experiments. The membranes were laboratory prepared. GO was prepared using the modified Hummer's method and added to a polyvinyl alcohol solution. In the authors' opinion, a novel GO membrane was successfully prepared and used as an effective adsorbent to selectively adsorb heavy metal ions – the maximum adsorption capacities of Cu^{2+}, Cd^{2+}, and Ni^{2+} were found to be 1.21, 0.81, and 1.08 mmol/g, respectively.

The paper of Liu et al. [28] summarizes the development and testing of novel GO membranes used for the removal of natural organic matter (NOM) from raw water sources. To fabricate the membrane (with 1 and 2 mg of GO), they used a commercial polyvinylidene fluoride (PVDF) membrane as the support layer. The trivalent cations Al^{3+} and Fe^{3+} were compared as crosslinking agents to enhance the stability of the GO nanosheets, which were stacked on the support membrane in the solution. It was found that the GO membrane crosslinked with Fe^{3+} provided a greater flux and NOM removal efficiency than the GO membrane crosslinked with Al^{3+} (approximately 1.1–2.3 times). For example, the flux of bovine serum albumin (BSA) solution was 35 L/m^2 h for Fe^3 and 15 L/m^2 h for Al^{3+} at crosslinking cations concentration 0.1 M each.

This research focuses on finding a basic polymer that would make the formation of membrane matrix possible. The requirements include good mechanical strength, compatibility with other polymers and organic solvents as well as good permeation properties. In the last decade, PVDF has become one of the more popular polymeric membrane materials because it is easily soluble in common organic solvents. This property allows for the production of porous membranes using phase inversion. When aqueous solutions are used in the permeation process, hydrophilicity of the membrane surface is important. Unfortunately, in refererence to other polymers, PVDF is relatively more hydrophobic [30]. However, the literature reports on the successful use of PVDF in the production of membranes [29–34].

Zhang et al. [35] proposed modification of PVDF membranes by oxidized carbon nanotubes (OMWNCTs), GO, and OMWNCTs/GO to improve their hydrophilicity and permeability. For PVDF/GO membrane, the contact angle decreased from 78.5° to 66.4°. The permeation flux increased by 17.23% comparing with PVDF membrane and the tensile strength increased from 1.866 to 2.106 MPa. The rejection of BSA (1 g/dm^3, under feed pressure 0.1 MPa) reached about 85.1%, while it was only 29.7% for the raw PVDF membrane.

The paper of Zhao et al. [36] presented results for PVDF/GO membrane. In the study, water flux tended to increase with the increase of GO content. When GO content was 2 wt%, water flux increased by 79% compared with pure PVDF membrane and contact angle decreased from 72.6° to 60.5°. In that paper BSA was used as an indicator for measuring

antifouling properties of membranes. It was observed that a larger amount of BSA was adsorbed on the original, raw PVDF membrane (165.11 mg/m^2) than on the membrane with GO (35.46 mg/m^2). The flux recovery ratio at ΔP = 0.1 MPa, 2 wt% GO, and 0.1 g/dm^3 BSA was approximately 90%.

On the basis of the discussed papers and earlier own research, the aim of this work was formulated. The objective of this study was to present the methodology of several membrane production methods, involving the application of different support layers as well as different nanoparticle distribution procedures. The resulting membranes were evaluated with regard to their thickness, elasticity, mechanical durability, the largest pore size, and hydrophilicity, and the latter was determined by measuring the contact angle. Manufactured membranes were tested in the ultrafiltration (UF) process using KOCH Membrane System equipment. Finally, the membranes produced with and without the addition of GO were characterized by calculating their permeation fluxes, mass transfer resistances, and BSA rejection rates from its solution.

2. Membrane preparation

The polymer matrix was formed from PVDF dissolved in dimethylacetamide (DMAC). Polyethylene glycol (PEG), of a molar mass of 200 g/mol, was added as a plasticizer. GO was used in the form of nanoflakes. The reagents and GO were purchased from Sigma-Aldrich, USA. The membranes were prepared via the phase inversion method, with or without the addition of GO.

100 g of the polymer solution contained 15 wt% PVDF and 5 wt% PEG, added as a plasticizer. An appropriate amount of PVDF, with a molar mass of 534,000 g/mol, was dissolved in DMAC, by magnetic stirring for 24 h at ambient temperature. The polymeric matrix was enriched by adding PEG (molar mass 200 g/mol) in order to improve its mechanical properties and plasticity. In this way, the basic polymeric mixture was prepared. The membrane was then formed with an Elcometer 3530 adjustable film applicator and conditioned in distilled water for about 24 h. When GO was added (2 mg), first it was ultrasonically dispersed in 10 g of DMAC for 1 h and combined with the polymer in different ways (described later).

Most studies involve the use of multilayer membranes containing a thin skin layer and a reinforced support in order to enhance their mechanical durability. Therefore, the additional support layer was produced from polysulfone (PSU) dissolved in dimethylformamide (DMF). As a result, porous membranes with or without GO were produced.

The GO membranes were produced in the following stages:

- Casting the solution of PSU and DMF as a support (about 150 μm). Preparation of the proper size support layer (about 30 × 30 cm) in order to determine the characteristics of three different parts of the prepared membrane and test the membrane in the UF process.
- Preparation of the PVDF solution according to the procedure described above.
- Formation of the membrane with GO, incorporated into the membrane via:
  - mixing (2 mg GO) with the whole volume of the polymer, and casting a thin layer (100 μm) of the polymer containing GO onto the basic crosslinked PSU layer (GO concentration in the membrane was 0.11 mg/cm^3 which corresponded to 0.002% content in membrane active layer),
  - spraying an ultrathin layer of GO (2 mg) dissolved in DMAC (5 cm^3) onto previously cast PVDF membrane.

The fabrication methods of three membranes are schematically shown in Fig. 1.

In the next stage of the study, membranes with PSU support and with or without the addition of GO were produced. Based on our own research, it was found that the membranes formed on the PSU support had the most favorable mechanical and permeation characteristics comparing with previously produced membranes without support. The layer configurations of the produced membranes are shown in Fig. 2.

3. Results and discussion

The developed membranes were evaluated by determining their thickness, contact angle, the largest pore size, and ultimate tensile strength. Membrane thickness was measured by Micro IP65, the contact angle was assessed using a Surftens-Universal apparatus (Optik Elektronik & Gerätetechnik mbH, Germany). Mechanical properties, that is, Young's modulus (MPa) and tensile strength at break (MPa) were determined with an Instron 3345 tester.

The measurement results are gathered in Table 1. Fig. 3 shows changes in the contact angle in relation to the method of introducing GO.

The permeability of the membranes was determined in the UF process using an OSMONICS KOCH apparatus operated at transmembrane pressures ranging from 0.1 to 0.6 MPa at 25°C. In the process, a membrane with an area A of 28.26 cm^2 was tested.

The volumetric permeation flux was calculated with Eq. (1) as follows:

$$J_v = \frac{V}{A \cdot t} \tag{1}$$

where J_v, volumetric permeation flux (m^3/(m^2 h)); V, permeate volume (m^3); A, membrane area (m^2); and t, time (h).

Knowing the permeation flux, the membrane resistance was determined from Eq. (2) as follows:

$$R_m = \frac{\Delta P}{J_v \cdot \eta} \tag{2}$$

where R_m, hydraulic resistance of the membrane (m^{-1}); ΔP, transmembrane pressure (Pa); and η, viscosity of water at 25°C (Pa s).

The largest pore size calculations were performed using the Bubble Point method [37]. The procedure is described in the standards of the American Society for Testing and Materials as Method F316 [38]. Pore diameters were determined from Eq. (3).

$$d = \frac{4 \cdot \sigma \cdot \cos\theta}{\Delta P} \cdot 10^{-6} \tag{3}$$

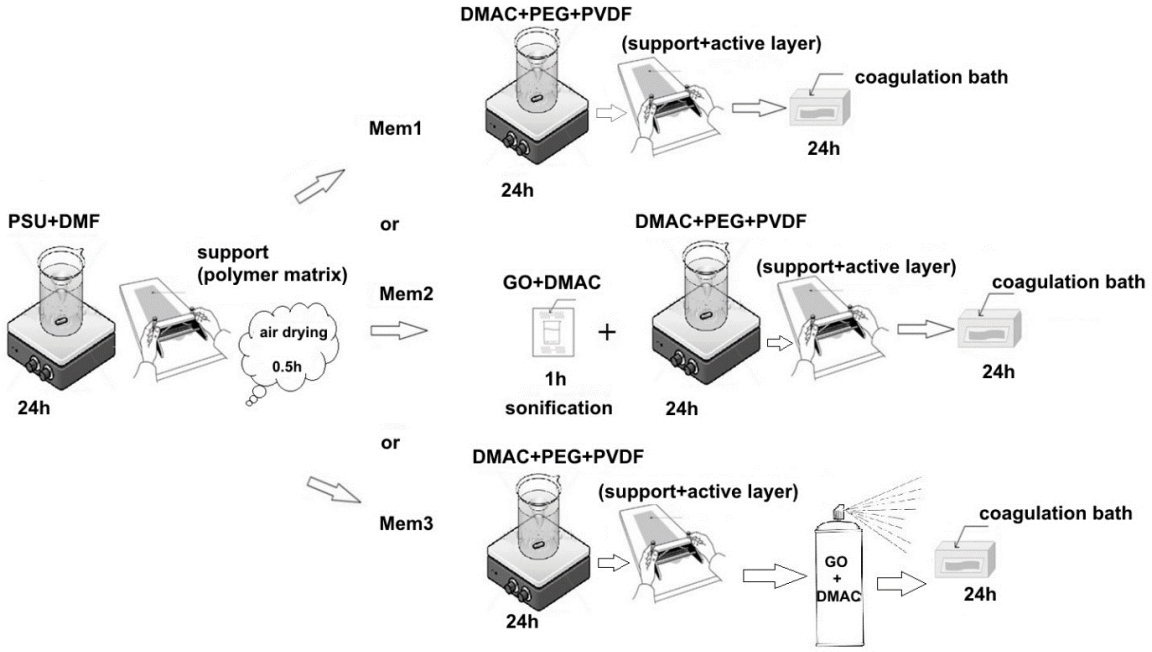

Fig. 1. Membrane preparation methods: Mem1, support and active layer without GO; Mem2, support and active layer with GO – mixing method; Mem3, support and active layer with GO – spraying method.

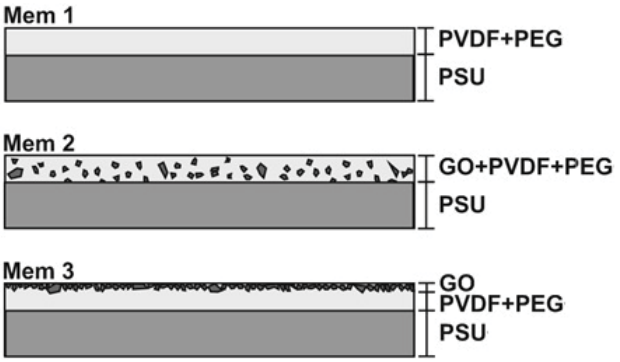

Fig. 2. Layer configurations of developed membranes.

where d, diameter of the largest pores in the membrane (μm); σ, water surface tension (N/m); and q, contact angle (°).

In the case of BSA separation, the retention coefficient was calculated from Eq. (4).

$$R = 1 - \frac{C_P}{C_R} \tag{4}$$

Fig. 3. Contact angle versus the method of GO location into the membrane: (a) without GO, (b) mixing with the polymer, and (c) applied via spraying.

where C_R, retentate concentration (g/dm^3) and C_P, permeate concentration (g/dm^3).

The total resistance R_T of a membrane system is the sum of the membrane R_m and the fouling R_F resistances (Eq. 5).

$$R_T = R_m + R_F \tag{5}$$

These resistances can be calculated from BSA permeation flux data and from the water flux through a clean membrane (Eq. (2)). As a result, it is possible to calculate the fouling resistance R_F.

Fig. 4 shows the water volumetric flux calculated for the membranes with and without GO. The flux (for ΔP = 0.6 MPa)

Table 1
Characteristics of the prepared membranes

Membrane	Thickness (μm)	Contact angle (°)	Young's modulus (MPa)	Tensile strength at break (MPa)	Largest pore size (μm)
Mem1	133 ± 6	72 ÷ 81	208 ± 22	0.024 ± 0.007	2.13 ÷ 2.24
Mem2	126 ± 3	59 ÷ 63	261 ± 27	0.084 ± 0.006	1.79 ÷ 2.05
Mem3	79 ± 6	10 ÷ 17	41 ± 17	0.021 ± 0.003	4.44 ÷ 4.57

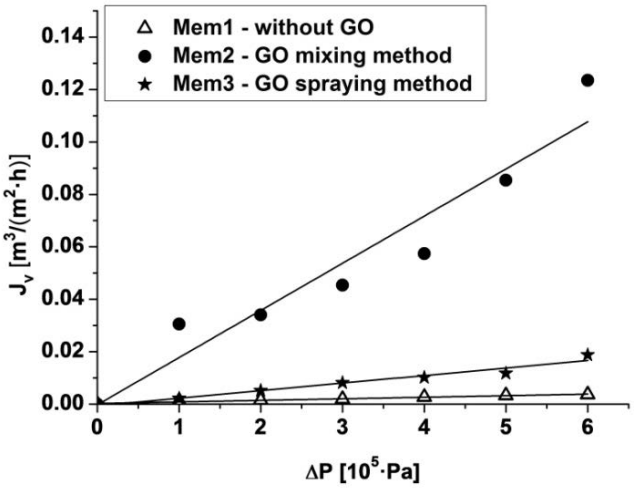

Fig. 4. Water volumetric flux for the membranes produced with and without the addition of GO versus transmembrane pressure.

through the membrane with GO distributed via spraying was lower (approaching J_v = 0.02 m^3/(m^2 h)) than that of the membrane produced via mixing (approaching J_v = 0.12 m^3/(m^2 h)). One possible explanation of this phenomenon is that the admixture of GO in the polymer matrix causes the formation of pores, which facilitates transport through Mem2. Comparing the permeability of Mem2 with Mem1 (for ΔP = 0.6 MPa) the volumetric flux increased approximately by 33-fold.

Fig. 5 illustrates the changes in a membrane resistance in relation to the transmembrane pressure for membranes with spraying and mixing GO introduction. The mass transfer resistance for the membrane obtained by the spraying is much higher than the one of the resaved by mixing. The spraying method does not decrease the resistance too much in relation to the reference membrane. Only the distribution of GO inside the membrane structure (PVDF + PEG) decreases the mass transfer resistance significantly.

Further stages of the study involved UF tests performed with a diluted solution of BSA (with a molecular weight of 66,430 Da) of concentrations of 0.5, 0.75, and 1.0 g/dm^3 at transmembrane pressures ranging from 1.0 to 6.0 × 10^5 Pa at 25°C. BSA was dissolved in 0.9% NaCl. The BSA content in the permeate and the retentate samples was determined by a spectrophotometric method (Thermo Fisher Scientific Spectrophotometer, λ = 279 nm). In this case, the tested membrane was produced by the mixing method (Mem2).

The volumetric flux was calculated with Eq. (1) and it is shown in Fig. 6. As expected, the fluxes obtained during BSA solutions filtrations depended on BSA concentration. The lowest value was obtained for the highest concentration. Fig. 7 illustrates the retention coefficient R determined for the analyzed solutions. The coefficient reached a value of R = 0.85, 0.89, and 0.93 for BSA concentrations equal to C_0 = 0.5, 0.75, and 1.0 g/dm^3, respectively.

Fig. 8 shows the total resistance R_T of the membrane for different BSA solutions similar to Fig. 5 pertaining to a "clean" membrane (Mem2). The fouling resistance of the membrane R_F shown in Fig. 9 was calculated using Eq. (5) assuming minimum (ΔP = 0.1 MPa) and maximum (ΔP = 0.6 MPa) transmembrane pressure.

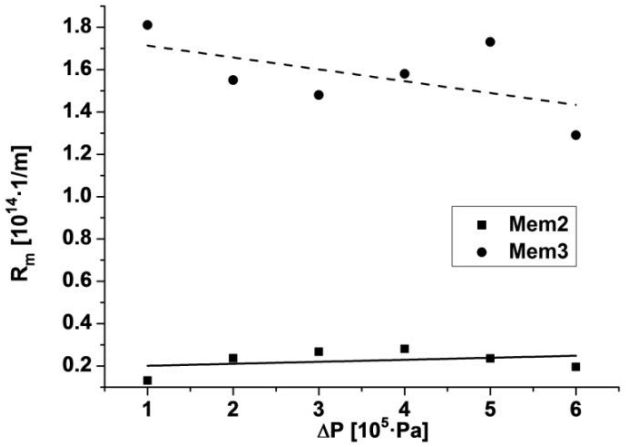

Fig. 5. The resistance of the membranes produced with the addition of GO versus transmembrane pressure.

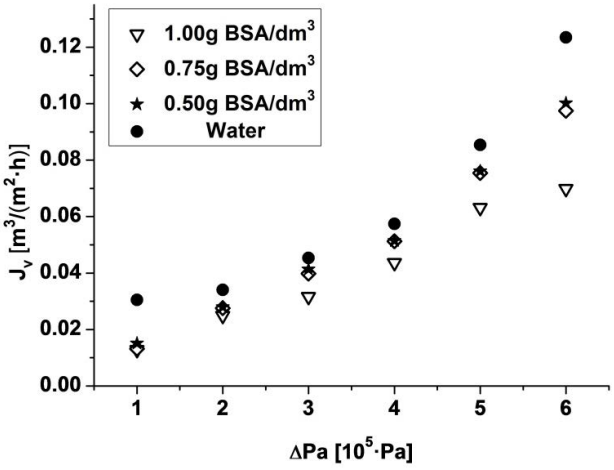

Fig. 6. Comparison of volumetric flux for different BSA concentrations for Mem2.

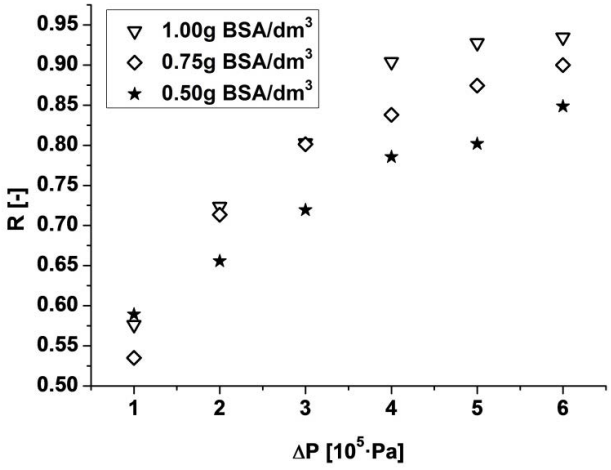

Fig. 7. Retention coefficient for different BSA concentrations for Mem2.

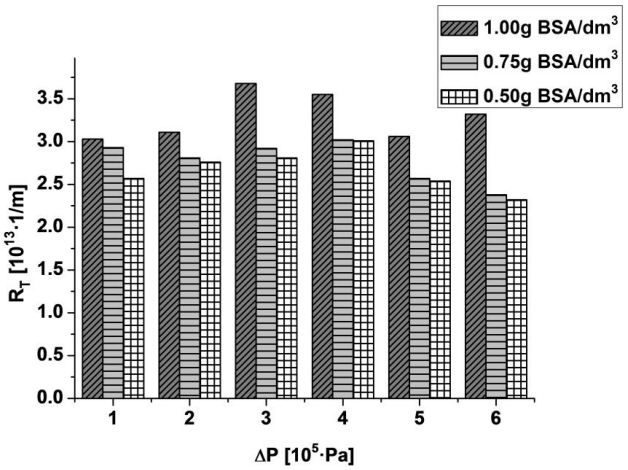

Fig. 8. Total resistance versus transmembrane pressure for Mem2.

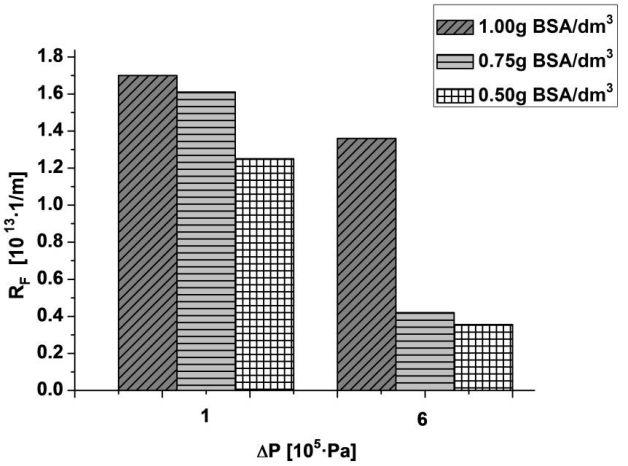

Fig. 9. Fouling resistance for different BSA concentrations versus transmembrane pressure.

4. Summary

The article attempts to explain the preparation of PVDF polymeric membranes via the phase inversion method and shows three possible configurations (including GO introduction) of the membranes preparation using the same components. The laboratory-scale production process resulted in elastic and mechanically durable membranes with the support layer made of PSU. Permeabilities of the produced membranes were compared by determining their volumetric permeation flux and resistance.

To summarize, the presence of GO in the membrane increased hydrophilicity of its surface, which was confirmed by measuring the contact angle. It was also discovered that the addition of GO significantly enhanced the membrane permeability.

Moreover, it was found that the addition of GO to the membrane structure by the mixing methods resulted in the highest improvement of the membrane permeability.

In the selected range of transmembrane pressures, poor permeation was detected for the PVDF membrane without GO and with the PSU support (J_v = 0.004 m^3/(m^2 h)). The membrane containing GO distributed in the whole volume of PVDF (mixing method) proved permeability toward water and provided higher fluxes (of up to J_v = 0.12 m^3/(m^2 h)), and the flux was higher than the one determined for the membrane containing GO distributed via spraying (approaching J_v = 0.02 m^3/(m^2 h)).

The laboratory-prepared functionalized GO/PVDF membranes with PSU support had an appropriate pore size distribution for the UF process, higher permeability as well as good BSA rejection, reaching over 90%.

The study shows that the proper addition of GO causes a substantial (up to a 33-fold) increase in the membrane permeability compared with the membranes without GO.

Symbols

A	—	Membrane area, m^2
C_0	—	Initial concentration, g/dm^3
C_P	—	Permeate concentration, g/dm^3
C_R	—	Retentate concentration, g/dm^3
d	—	Diameter of the largest pores in the membrane, μm
J_v	—	Volume flux, m^3/(m^2 h)
R	—	Retention coefficient, –
R_F	—	Fouling resistance, m^{-1}
R_m	—	Hydraulic resistance of the membrane, m^{-1}
R_T	—	Total resistance, m^{-1}
t	—	Time, h
V	—	Permeate volume, m^3
ΔP	—	Transmembrane pressure, Pa
q	—	Contact angle, °
η	—	Viscosity of water at 25°C, Pa s
σ	—	Surface tension, N/m

References

[1] L.M. Camacho, L. Dumée, J. Zhang, J. Li, M. Duke, J. Gomez, S. Gray, Advances in membrane distillation for water desalination and purification applications, Water, 5 (2013) 94–196.
[2] S. Yarlagadda, L.M. Camacho, V.G. Gude, Z. Wei, S. Shuguang Deng, Membrane distillation for desalination and other separations, Recent Pat. Chem. Eng., 2 (2009) 128–158.
[3] I.-G. Yi, J.-K. Kang, J.-H. Kim, S.-C. Lee, E.-H. Sim, J.-A. Park, S.-B. Kim, Adsorption characteristics of graphene oxide in the removal of Cu(II) from aqueous solutions, Desal. Wat. Treat., 72 (2017) 308–317.
[4] J. Wang, N. Li, Y. Zhao, S. Xia, Graphene oxide modified semi-aromatic polyamide thin film composite membranes for PPCPs removal, Desal. Wat. Treat., 66 (2017) 166–175.
[5] N.C. Muller, B. Burgen, V. Kueter, P. Luis, T. Melin, W. Pronk, R. Reseiwitz, D. Rickerby, G.M. Rios, W. Wennekes, B. Nowack, Nanofiltration and nanostructured membranes – should they be considered nanotechnology or not? J. Hazard. Mater., 211–212 (2012) 275–280.
[6] M. Sadeghi, M.A. Semsarzadeh, H. Moadel, Enhancement of the gas separation properties of polybenzimidazole (PBI) membrane by incorporation of silica nano particles, J. Membr. Sci., 331 (2009) 21–30.
[7] J. Hong, Y. He, Effects of nano sized zinc oxide on the performance of PVDF microfiltration membranes, Desalination, 302 (2012) 71–79.
[8] P. Sun, M. Zhu, K. Wang, M. Zhong, J. Wei, D. Wu, Z. Xu, H. Zhu, Selective ion penetration of graphene oxide membranes, Nano, 22 (2013) 428–437.
[9] K.W. Putz, O.C. Compton, M.J. Palmeri, S.T. Nguyen, L.C. Brinson, High nanofiller content graphene oxide–polymer

nanocomposites via vacuum assisted self-assembly, Adv. Funct. Mater., 20 (2010) 3322–3329.
[10] N. Wei, X. Peng, Z. Xu, Understanding water permeation in graphene oxide membranes, ACS Appl. Mater. Interface, 6 (2014) 5877–5883.
[11] M. Blus, E. Tomczak, Hydrodynamics of ultrafiltration polymer membranes with carbon nanotubes, Desal. Wat. Treat., 64 (2017) 298–301.
[12] A. Anand, B. Unnikrishnan, J.-Y. Mao, H.-J. Lin, C.-C. Huang, Graphene-based nanofiltration membranes for improving salt rejection, water flux and antifouling – a review, Desalination, 429 (2018) 119–133.
[13] C.K. Chua, M. Pumera, Chemical reduction of graphene oxide: a synthetic chemistry viewpoint, Chem. Soc. Rev., 7 (2014) 291–312.
[14] Y. Han, Y. Jiang, C. Gao, High-flux graphene oxide nanofiltration membrane intercalated by carbon nanotubes, ACS Appl. Mater. Interfaces, 7 (2015) 8147–8155.
[15] W.S. Hummers, R.E. Offeman, Preparation of graphitic oxide, J. Am. Chem. Soc., 80 (1958) 339.
[16] R.K. Joshi, P. Carbone, F.C. Wang, V.G. Krevets, Y. Su, I.V. Grigorieva, H.A. Wu, A.K. Geim, R.R. Nair, Precise and ultrafast molecular sieving trough graphene oxide membranes, Science, 343 (2014) 752–754.
[17] A. Nicolai, B.G. Sumpter, V. Meuniera, Tunable water desalination across graphene oxide framework membranes, Phys. Chem. Chem. Phys., 16 (2014) 8646–8654.
[18] S. Xia, M. Ni, Preparation of poly(vinylidene fluoride) membranes with graphene oxide addition for natural organic matter removal, J. Membr. Sci., 473 (2015) 54–62.
[19] E. Saljoughi, M. Sadrzadeh, T. Mohammadi, Effect of preparation variables on morphology and pure water permeation flux through asymmetric cellulose acetate membranes, J. Membr. Sci., 326 (2009) 627–634.
[20] H.M. Hegab, Y. Wimalasiri, M. Ginic-Markovic, L. Zou, Improving the fouling resistance of brackish water membranes via surface modification with graphene oxide functionalized chitosan, Desalination, 365 (2015) 99–107.
[21] L. Wu, Z. Qin, F. Yu, J. Ma, Graphene oxide cross-linked chitosan nanocomposite adsorbents for the removal of Cr (VI) from aqueous environments, Desal. Wat. Treat., 72 (2017) 300–307.
[22] B. Fryczkowska, D. Biniaś, C. Ślusarczyk, J. Fabia, J. Janicki, Influence of graphene oxide on the properties of composite polyacrylonitrile membranes, Desal. Wat. Treat., 81 (2017) 67–79.
[23] H.M. Hegab, L. Zou, Graphene oxide-assisted membranes: fabrication and potential applications in desalination and water purification, J. Membr. Sci., 484 (2015) 95–106.
[24] B. Mi, Graphene oxide membranes for ionic and molecular sieving, Science, 343 (2014) 740–742.
[25] M. Hosseini, J. Azamat, H. Erfan-Niya, Improving the performance of water desalination through ultra-permeable functionalized nanoporous graphene oxide membrane, Appl. Surf. Sci., 427 (2018) 1000–1008.
[26] X. Wang, X. Wang, P. Xiao, J. Li, E. Tian, Y. Zhao, Y. Ren, High water permeable free-standing cellulose triacetate/graphene oxide membrane with enhanced antibiofouling and mechanical properties for forward osmosis, Colloids Surf., A, 508 (2016) 327–335.
[27] P. Tan, Y. Hu, Q. Bi, Competitive adsorption of Cu^{2+}, Cd^{2+} and Ni^{2+} from an aqueous solution on graphene oxide membranes, Colloids Surf., A, 509 (2016) 56–64.
[28] T. Liu, B. Yang, N. Graham, W. Yu, K. Sun, Trivalent metal cation cross-linked graphene oxide membranes for NOM removal in water treatment, J. Membr. Sci., 542 (2017) 31–40.
[29] J. Zahirifara, J. Karimi-Sabet, S. Mohammad Ali Moosaviana, A. Hadi, P. Khadiv-Parsi, Fabrication of a novel octadecylamine functionalized graphene oxide/PVDF dual-layer flat sheet membrane for desalination via air gap membrane distillation, Desalination, 428 (2018) 227–239.
[30] K.-J. Lu, J. Zuo, T.-S. Chung, Novel PVDF membranes comprising n-butylamine functionalized graphene oxide for direct contact membrane distillation, J. Membr. Sci., 539 (2017) 34–42.
[31] R.K. Joshi, S. Alwarappan, M. Yoshimura, V. Sahajwalla, Y. Nishina, Graphene oxide: the new membrane material, Appl. Mater. Today, 1 (2015) 1–12.
[32] S. Ayyaru, Y.-H. Ahn, Application of sulfonic acid group functionalized graphene oxide to improve hydrophilicity, permeability, and antifouling of PVDF nanocomposite ultrafiltration membranes, J. Membr. Sci., 525 (2017) 210–219.
[33] W. Miao, Z.-K. Li, X. Yan, Y.-J. Guo, W.-Z. Lang, Improved ultrafiltration performance and chlorine resistance of PVDF hollow fiber membranes via doping with sulfonated graphene oxide, Chem. Eng. J., 317 (2017) 901–912.
[34] Z. Zhu, L. Wang, Y. Xu, Q. Li, J. Jiang, X. Wang, Preparation and characteristics of graphene oxide-blending PVDF nanohybrid membranes and their applications for hazardous dye adsorption and rejection, J. Colloid Interface Sci., 504 (2017) 429–439.
[35] J. Zhang, Z. Xu, W. Mai, C. Min, B. Zhou, M. Shan, Y. Li, C. Yang, Z. Wang, X. Qian, Improved hydrophilicity, permeability, antifouling and mechanical performance of PVDF composite ultrafiltration membranes tailored by oxidized low-dimensional carbon nanomaterials, J. Mater. Chem. A, 1 (2013) 3101–3111.
[36] C. Zhao, X. Xu, J. Chen, F. Yang, Effect of graphene oxide concentration on the morphologies and antifouling properties of PVDF ultrafiltration membranes, J. Environ. Chem. Eng., 1 (2013) 349–354.
[37] G. Reichelt, Patent Number 4,744,240, Method for Determining the Bubble Point or the Largest Pore of Membranes or Filter Materials, US Patent, 1988.
[38] Standard Test Method for Pore Size Characteristics of Membrane Filters by Bubble Point and Mean Flow Pore Test, ASTM International, West Conshohocken, PA, 3, 2011.